

Supporting information for:
**Defect Dominated Charge Transport and Fermi
Level Pinning in MoS₂/Metal Contacts**

Pantelis Bampoulis,^{*,†,‡} Rik van Bremen,[†] Qirong Yao,[†] Bene Poelsema,[†] Harold
J. W. Zandvliet,[†] and Kai Sotthewes^{*,†}

[†] *Physics of Interfaces and Nanomaterials, MESA+ Institute for Nanotechnology,
University of Twente, P.O.Box 217, 7500AE Enschede, The Netherlands.*

[‡]*Physics of Fluids and J.M. Burgers Centre for Fluid Mechanics, MESA+ Institute for
Nanotechnology, University of Twente, P.O.Box 217, 7500AE Enschede, The Netherlands.*

E-mail: p.bampoulis@utwente.nl; k.sotthewes@utwente.nl

SI-1. Experimental Configuration

The contact geometry is shown in the schematic of S1. A micrometer thick and millimeter wide MoS₂ flake (freshly cleaved) is placed on top of a mica substrate. The mica substrate provides mechanical stability, which is highly desired during the C-AFM measurements. The electrical contact of the MoS₂ flake is achieved via a graphite flake that is attached to one end of the MoS₂ flake. The graphite flake is a few millimeters wide. The C-AFM measurements were conducted with p-doped diamond/PtSi/n-doped Si tips in contact mode. The conductive tip is grounded and the bias voltage was applied to the graphite electrode. In this work we refer to forward bias when the sample is negatively biased relative to the tip and vice versa for the reverse bias regime.

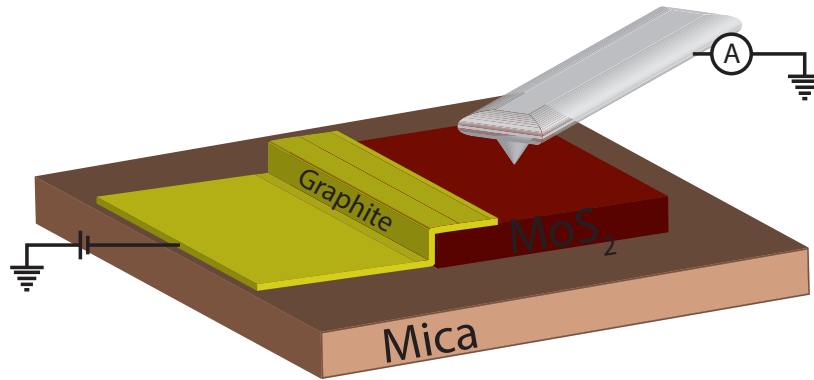


Figure S1: Schematic diagram of the C-AFM configuration. A micrometer thick MoS₂ flake is placed on top of a supporting mica substrate. The mica substrate provides mechanical stability. A large graphite flake (millimeters wide) makes electrical contact with the MoS₂.

SI-2. Water Adsorption and Desorption

The experiments were performed in N₂ environment. In this environment the relative humidity (RH) was measured to be below 1%. We have previously shown^{S1} that water adsorption on MoS₂, only occurs at high relative humidity (~75%). Typically samples prepared and measured at ambient relative humidity do not show any sign of adsorbed water structures, except for the occasional appearance of nanodroplets at MoS₂ defect sites. We have shown

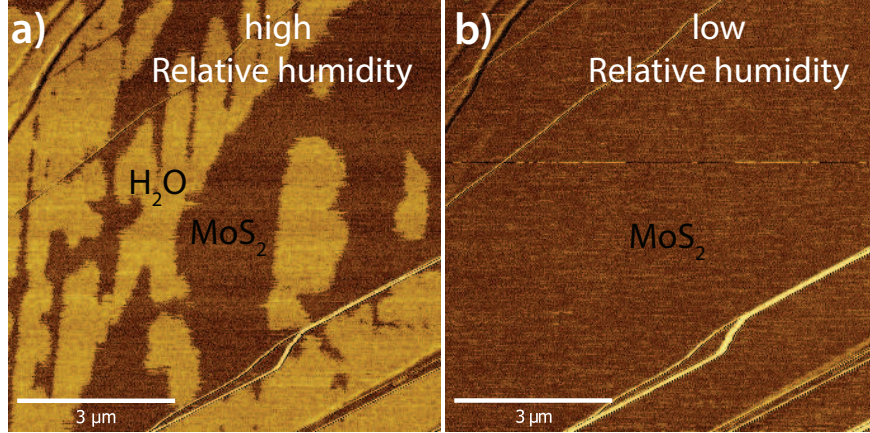


Figure S2: (a) Phase image (tapping mode) of MoS₂ covered with water layers (bright contrast). The water layers were formed when the surface was exposed to $\sim 75\%$ RH and they disappear when we reduce the RH below 10%, panel (b).

that these water structures evaporate from the surface when the RH is decreased below 10%.^{S1}

Figure S2a shows a phase image obtained by tapping mode AFM. Two distinct contrast levels are observed. The brighter contrast appeared only when the sample was exposed to $\sim 75\%$ for a couple of minutes and is attributed to the presence of water on the surface. These water layers immediately disappear from the surface when the humidity of the AFM chamber drops below $<10\%$, see figure S2b. The C-AFM measurements shown in this work were performed at RH $<1\%$, at this RH the presence of water on the surface is excluded. This ensures that our measurements are not influenced by the presence of water.

SI-3. Comparison Between Metal-like Defects and Sulfur Vacancies Measured by STM and AFM

Figure S3a shows a large scale C-AFM image of the MoS₂ surface. The surface is covered with metal-like defects, i.e., the dark depressions in the image. In C-AFM images we see two types of defects, that are categorized by the amplitude of the current at their center. These defects fall into two categories, defects that originate from the first MoS₂ trilayer, dark

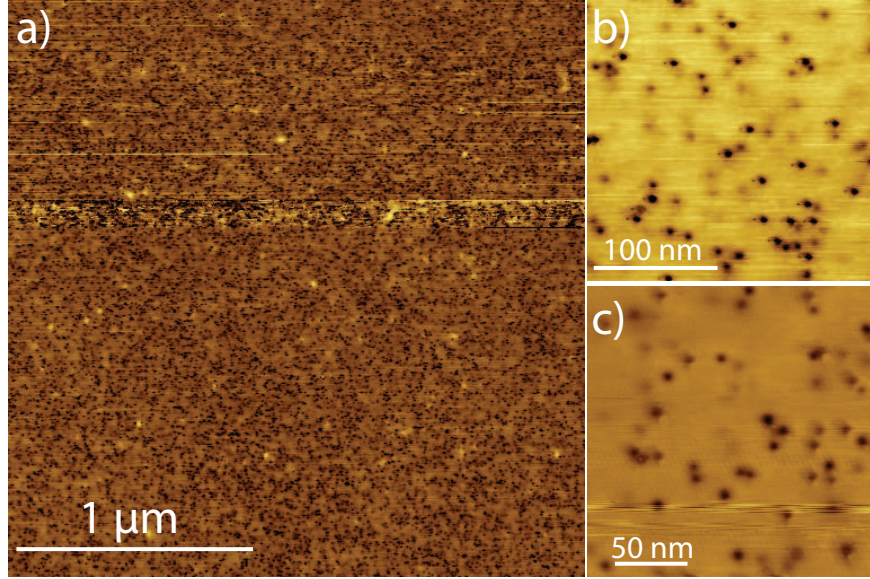


Figure S3: (a) Large scale C-AFM image of MoS₂. The surface is covered with metal-like defects (dark depressions). (b) A smaller C-AFM image revealing two types of dark defects, deep dark and faint dark depressions. The faint dark depressions are defects in the second MoS₂ trilayer, whereas the deep dark defects are situated in the top MoS₂ trilayer. (c) STM image revealing the same two type of defects with the same contrast variations (setpoint = 0.1 nA and 0.2 V).

depressions in figure S3b, and defects arising from the second MoS₂ trilayer, faint depressions in figure S3b. In order to obtain further structural information on the metal-like defects we have performed STM measurements on the same sample. We see that also in STM images two types of defects are found across the surface, Figure S3c. Again two contrast levels are observed in line with the C-AFM measurements. The defect number density of the darker depressions accounts to approximately $((0.8 \pm 0.2) \times 10^{11} \text{ cm}^{-2})$, a value very close to that found in the C-AFM measurements $((0.6 \pm 0.3) \times 10^{11} \text{ cm}^{-2})$.

In the main text we have argued that S-vacancies are not the cause of the dark round features (depressions at positive sample bias), i.e., metal-like defects. S-vacancies can be found all over the surface, and they do not substantially influence their surroundings. We have obtained atomic resolution STM images of S-vacancies, similar to the one shown in Figure S4a. From such images we obtain a density of $(0.7 \pm 0.4) \times 10^{13} \text{ cm}^{-2}$ which is 2 orders of magnitude larger than the number density of the metal-like defects $((0.8 \pm 0.2) \times 10^{11}$

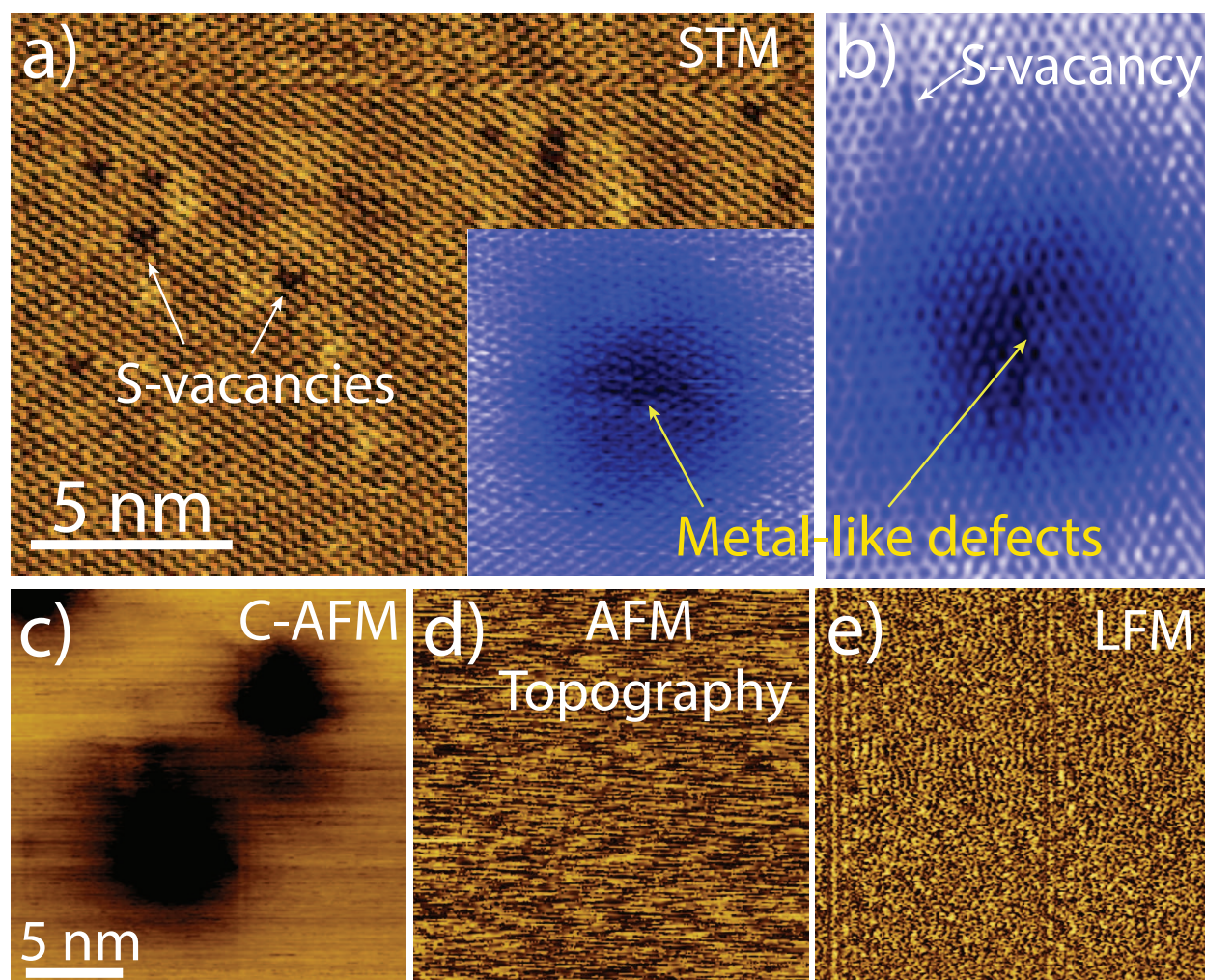


Figure S4: (a) STM image showing multiple S-vacancies of the outermost S layer. The S-vacancies do not induce any substantial changes on their environment in direct contrast to the metal-like defects (setpoint -0.3 V and 0.4 nA). Inset: metal-like defect measured with STM (setpoint: -1.8 V and 0.4 nA). (b) STM image showing a S-vacancy and a metal-like defect (setpoint: -1.8 V and 0.4 nA). (c) C-AFM image of metal-like defects, (d) and (e) the simultaneously recorded topography and LFM images of the same location, showing no apparent contrast.

cm^{-2}). High resolution STM images of the metal-like defects show that S-vacancies alone cannot be the cause of their appearance, see the inset of figure S4a. This is clear in figure S4b where we have captured within the same image a metal-like defect and a S-vacancy.

In addition, it is evident from images, like those shown in Figure 1b of the main text and Figure S4c, that the defects are only present in the C-AFM images, suggesting that they are electronic in nature. AFM topography and LFM images indicate that a missing S-atom fragment is unlikely; such a structural defect should give rise to a strong contrast in both the AFM topography and the lateral force signal. However, this is not the case, both the AFM topography and LFM image, for instance in Figure 1a of the main text and Figure S4d and e, show smooth surfaces, i.e., free of any structural defects. We would like to emphasize that AFM and LFM, and unlike STM, are not influenced by the electronic properties of the surface. The AFM topographic image (up to some extent) can be considered to represent the real surface topography and the LFM image can give material contrast. In both images the surface is smooth and homogeneous, i.e., free of any structural surface defects and the tip (according to the LFM images) interacts everywhere with the same surface. In contrast the simultaneously recorded C-AFM images, Figure 1b of the main text and Figure S4c, provide us information about the electronic structure across the surface.

SI-4. Non-destructive Measurements

Figure S5 shows two consecutive small scale lateral force microscopy (LFM) images obtained with 20 nN tip load. Atomic periodicity can be measured in both images due to the stick and slip motion of the AFM tip, this is clearly shown in the low pass filtered images of the insets of Figure S5. The stick and slip motion is homogeneous across the whole scanned area in both images, indicating that the imaging conditions are non-destructive. In both cases the tip interacts with the periodic surface of MoS_2 .

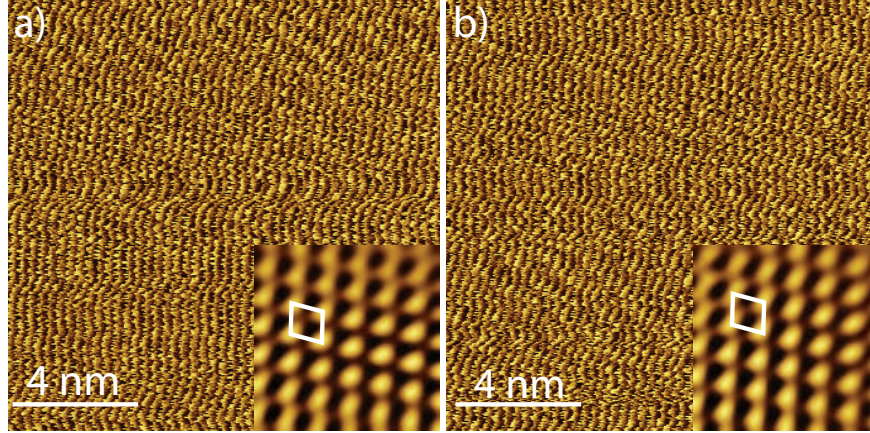


Figure S5: (a-b) Consecutive LFM images of MoS₂ obtained with 20 nN tip load. Both images clearly show stick and slip motion with atomic periodicity that matches the lattice constant of MoS₂. insets: atomic scale low pass filtered images of the respective LFM images, showing a clear hexagonal symmetry with a periodicity of 0.31 nm, i.e., close to the MoS₂ lattice constant.

SI-5. Inverse FFT and Striped Phase

The Fast Fourier Transform (FFT) as displayed in Figure S6a shows not only hexagonal symmetry, but also shows two strong peaks with a larger periodicity (~ 38 nm). The observation of these two strong spots in the FFT pattern indicates the presence of a one-dimensional striped phase. The occurrence of the striped phase (marked with white circles in Figure S6a and shown in the inverse FFT of Figure S6b) might be due to the relatively large effective areal coverage of the defects. The defects, which have most probable nearest neighbour distance of ~ 19 nm, have a density of $\sim 10^{11}$ cm⁻² resulting into an effective coverage of ~ 0.3 . In 1995 Ng and Vanderbilt^{S2} investigated the energetic ground states of a model two-phase system with electrostatic, magnetostatic or elastic $1/r^3$ dipolar interactions in two dimensions. At low and high coverages ($0 < \theta < 0.286$ and $0.714 < \theta < 1$) they found a droplet and an inverted droplet phase, respectively. In the intermediate range, i.e. $0.286 < \theta < 0.714$ the authors found a striped phase. This model may give a hint for understanding our observed striped phase. A more definite conclusion requires a systematic variation of the defect density, which is out of reach in our natural samples.

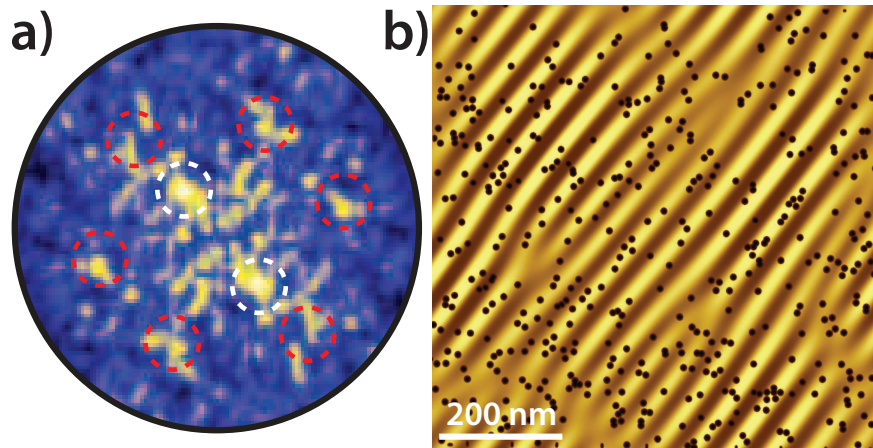


Figure S6: (a) The FFT spectra created from Figure 1b by considering the centers of the defects. The FFT not only reveals a hexagonal symmetry (red circles) with a periodicity of ~ 19 nm but also a one dimensional feature (white circles). (b) Guide to the eye of the 1D feature observed in panel (a). The black circles represent the position of the defects in Figure 1b. This Figure is the result of the inverse FFT of the selected Fourier components (1D spots marked with the white dashed circles) overlaid with the locations of the defects. A clear correlation between the bright stripes and the locations of the defects is observed.

References

- (S1) Bampoulis, P.; Teernstra, V. J.; Lohse, D.; Zandvliet, H. J.; Poelsema, B. Hydrophobic Ice Confined between Graphene and MoS₂. *J. Phys. Chem. C* **2016**, *120*, 27079–27084.
- (S2) Ng, K.-O.; Vanderbilt, D. Stability of Periodic Domain Structures in a Two-Dimensional Dipolar Model. *Phys. Rev. B* **1995**, *52*, 2177–2183.